ELSEVIER

Physica D 158 (2001) 45–68

PHYSICA D

www.elsevier.com/locate/physd

Sideband instabilities and defects of quasipatterns

Blas Echebarria*, Hermann Riecke

Department of Engineering Sciences and Applied Mathematics, Northwestern University, 2145 Sheridan Road, Evanston, IL 60208, USA

Received 27 December 2000; received in revised form 17 July 2001; accepted 17 July 2001
Communicated by F.H. Busse

Abstract

Quasipatterns have been found in dissipative systems ranging from Faraday waves in vertically vibrated fluid layers to nonlinear optics. We describe the dynamics of octagonal, decagonal and dodecagonal quasipatterns by means of coupled Ginzburg–Landau equations and study their stability to sideband perturbations analytically using long-wave equations as well as by direct numerical simulation. Of particular interest is the influence of the phason modes, which are associated with the quasiperiodicity, on the stability of the patterns. In the dodecagonal case, in contrast to the octagonal and the decagonal case, the phase modes and the phason modes decouple and there are parameter regimes in which the quasipattern first becomes unstable with respect to phason modes rather than phase modes. We also discuss the different types of defects that can arise in each kind of quasipattern as well as their dynamics and interactions. Particularly interesting is the decagonal quasipattern, which allows two different types of defects. Their mutual interaction can be extremely weak even at small distances.

PACS: 47.54·+r; 47.20.Ky; 47.35·+i; 61.44.Br

Keywords: Quasipatterns; Ginzburg–Landau equations; Phase equation; Sideband instabilities; Defects

1. Introduction

Since the discovery of quasicrystals in 1984 [1], much attention has been paid to the properties of these materials. In contrast to perfect crystals they lack periodicity, but preserve long-range orientational order. Due to this lack of periodicity quasicrystals may have noncrystallographic rotational symmetry and, in fact, materials have been found with 5-, 8-, 10- or 12-fold rotational axes.

In dissipative systems, the possibility of quasiperiodic structures, or quasipatterns, was also suggested some time ago [2]. Since then they have been observed in Faraday waves with one- and two-frequency forcing [3,4] and in nonlinear optics [5]. Marangoni convection with a deformable interface has been suggested to support quasipatterns [6], although they have not been observed so far. They have also been predicted in a model for the deformation of thin films subjected to laser irradiation [7].

* Corresponding author. Present address: Physics Department, Northeastern University, Boston, MA 02115, USA. Tel.: +1-617-373-2924; fax: +1-617-373-2943.
E-mail addresses: blas@presto.physics.neu.edu (B. Echebarria), h-riecke@northwestern.edu (H. Riecke).

0167-2789/01/$ – see front matter
PII: S0167-2789(01)00319-0

In Faraday waves, a great variety of patterns has been observed. They include superlattices, rhombic states, oscillons, as well as quasipatterns [8–10]. While quasipatterns are nonperiodic structures, superlattices are periodic in a scale larger than the critical wavelength of the system. In order for superlattices and quasipatterns to be stable, the mutual suppression of plane-wave modes of different orientation has to be sufficiently weak. This can be due to a few, somewhat different mechanisms. When forced with two frequencies, the system can exhibit simultaneously instabilities at two different wavelengths and the quasipatterns and superlattices appear near this bicritical point. The angle between the wavevectors of the destabilizing modes depends on the ratio of the two wavelengths. It determines whether the resulting patterns corresponds to a superlattice or a quasipattern. A mechanism involving two length scales was suggested sometime ago for quasicrystals [11] and studied in dissipative systems by means of a modified Swift–Hohenberg equation with two marginal modes [12]. The second length scale need not be associated with a proper instability. It can be sufficient that one of the modes is weakly damped. The interaction of the unstable mode with this damped mode can then lead to a reduction in the mutual suppression of modes subtending a certain angle [13]. Alternatively, the interaction with the damped mode can strongly enhance the saturating self-coupling term which then effectively leads to a reduction of the competition over a wide range of angles [14,15]. This favors patterns with a large number of modes. Calculations of the coefficients of the amplitude equations for Faraday waves suggest that this is indeed the case [16,17].

In nonlinear optics, the optical field in a nonlinear cavity can be rotated in order to obtain a structure with the desired number of modes [5]. In these systems, it is also possible to arrange patterns with two different spatial scales, leading to complex quasicrystalline structures [18–20]. However, dodecagonal quasipatterns have been observed in optical systems even with continuous rotational symmetry [21].

The relative stability of perfect quasipatterns has already been addressed [2]. In the present paper, we are interested in the stability of n-fold quasipatterns to sideband perturbations, in particular to slowly varying modulations. We will assume that the physical fields can be expanded as a sum of Fourier modes rotated by $2\pi/n$ relative to each other (similar to the density wave picture of quasicrystals), with slowly varying amplitudes in space and time. Using symmetry arguments, we determine a set of coupled Ginzburg–Landau equations for these amplitudes. Due to the lack of periodicity, a rigorous derivation from the basic equations using a center manifold reduction has not been possible so far. Thus, we consider the Ginzburg–Landau equations as phenomenological models and obtain general, analytical expressions for the stability of quasipatterns that can be applied to specific problems and compared with experiments.

As is well known in the study of quasicrystals, the long-wave dynamics of the system is governed by two types of modes: phonons and phasons. The former ones are marginal modes arising from spatial translation symmetries. The phasons, on the other hand, are additional marginal modes characteristic of quasicrystals and appear because of the quasiperiodic nature of these structures. Similarly, in the case of two-dimensional quasipatterns, the phases can be split into two subsets, according to their transformation properties. There are the two usual phase modes related to translations in space and, in addition, phason modes, corresponding to internal rearrangements in the pattern. As we will see later, in octagonal and dodecagonal quasipatterns the latter modes have a very simple geometrical interpretation. Since these quasipatterns can be viewed as two superimposed square (hexagonal) lattices rotated by $2\pi/8$ ($2\pi/12$), the phason modes correspond to *relative* translations between the two lattices. It is worth mentioning that when the angle between the two lattices satisfies certain conditions, the whole structure becomes periodic with a wavelength larger than that of the individual lattices. The resulting patterns are known as superlattices [22]. In this case, extra resonance conditions among the modes are satisfied [23], and the phason modes become damped and can, in principle, be eliminated in a long-wave analysis.

This paper is organized as follows. In the next three sections, we study octagonal, decagonal and dodecagonal quasipatterns arising from steady bifurcations. In each case, we start with the amplitude equations and study various simple solutions and their relative stability. Our main focus is the long-wave dynamics of the quasiperiodic

solutions. We derive coupled equations for the phase and phason modes, obtaining the diffusive counterpart to the elastic equations for a quasicrystal [24]. We then calculate the long-wave stability limits for sideband perturbations and investigate numerically the behavior arising from the instabilities. In Section 5, we discuss the different types of defects that appear in each kind of quasipattern and their dynamics and interactions. Conclusions are presented in Section 6.

2. Octagonal quasipatterns

2.1. Ginzburg–Landau equations

We consider a quasipattern composed of four modes, $\psi = \eta\sum_{n=1}^{4} A_n(\mathbf{x}, t)\, \mathrm{e}^{\mathrm{i}\mathbf{k}_n\cdot\hat{\mathbf{x}}} + \text{c.c.} + \text{h.o.t.}$, where $\eta \ll 1$ and the amplitudes $A_i(\mathbf{x}, t)$ satisfy the equations (after rescaling):

$$\partial_t A_i = \mu A_i + (\hat{\mathbf{n}}_i \cdot \nabla)^2 A_i - A_i[|A_i|^2 + \nu|A_{i+2}|^2 + \gamma(|A_{i+1}|^2 + |A_{i+3}|^2)] \tag{1}$$

with μ the control parameter and $\hat{\mathbf{n}}_i$ the unit vector in the direction of the wavenumber $\mathbf{k}_i$ (see Fig. 1a). The amplitudes A_i depend on slow scales $x = \eta\hat{x}$ and $t = \eta^2\hat{t}$. Here and in the following, the indices are repeated cyclically with period 4. Thus, A_5 corresponds to A_1, etc. The coefficients ν and γ measure the interaction between modes that subtend an angle of $\pi/2$ and $\pi/4$, respectively.

Eq. (1) has gradient structure

$$\partial_t A_i = -\frac{\partial \mathcal{F}}{\partial \bar{A}_i}, \tag{2}$$

and can be derived from the Lyapunov functional

$$\mathcal{F} \equiv \iint \mathrm{d}x\,\mathrm{d}y\, F = \iint \mathrm{d}x\,\mathrm{d}y \sum_{i=1}^{4}\left[-\mu|A_i|^2 + |(\hat{\mathbf{n}}_i\cdot\nabla)^2 A_i|^2 + \frac{1}{2}|A_i|^4 + \gamma|A_i|^2|A_{i+1}|^2 + \frac{\nu}{2}|A_i|^2|A_{i+2}|^2\right]. \tag{3}$$

Therefore, the dynamics of the system are relaxational.

In order to calculate the different solutions, we write $A_j = a_j\, \mathrm{e}^{\mathrm{i}\phi_j}$, with a_j real. Splitting into real and imaginary parts yields

$$\partial_t a_i = \mu a_i - a_i[a_i^2 + \nu a_{i+2}^2 + \gamma(a_{i+1}^2 + a_{i+3}^2)], \tag{4}$$

$$\partial_t \phi_i = 0. \tag{5}$$

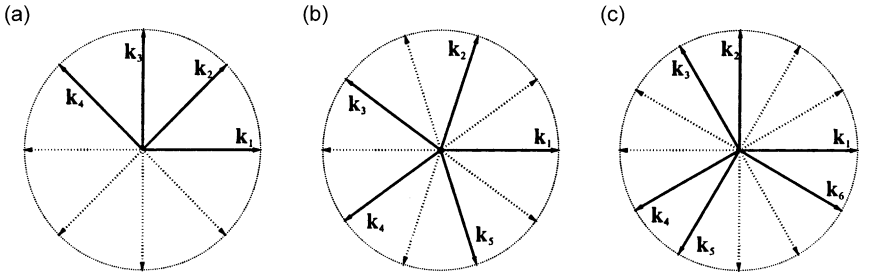

Fig. 1. Fourier modes composing the (a) octagonal, (b) decagonal, and (c) dodecagonal quasipatterns. Solid vectors denote the modes described by Eqs. (1), (41), (87) and (88), respectively.

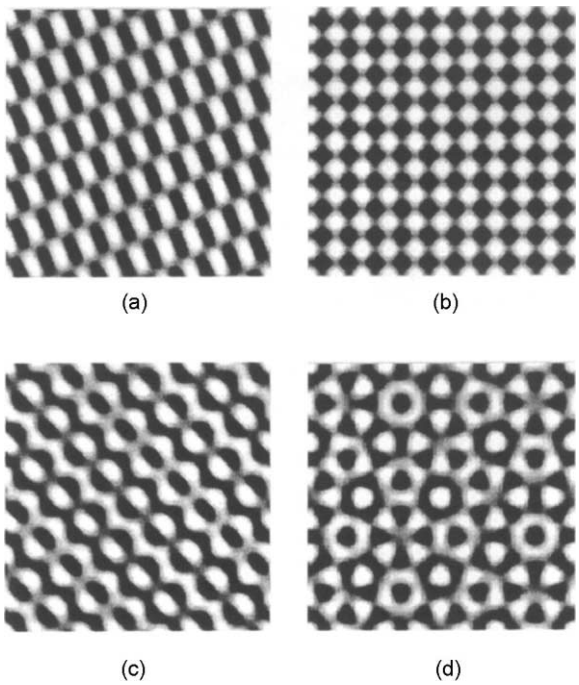

Fig. 2. Octagonal case. Different types of solutions of Eq. (1) obtained by reconstructing the physical field ψ from the amplitudes A_i: (a) rectangles, (b) squares, (c) 1D quasipattern, and (d) octagonal quasipattern.

The amplitudes can be considered to be real ($\phi_1 = \cdots = \phi_4 = 0$). There are five different kinds of simple solutions [2] (see Fig. 2):

1. Rolls: $a_2 = a_3 = a_4 = 0$ and $a_1 = \sqrt{\mu}$. The value of the Lyapunov functional for rolls is: $F_{\mathrm{R}} = -\frac{1}{2}\mu^2$.
2. Squares: $a_2 = a_4 = 0$ and $a_1 = a_3 = \sqrt{\mu/(\nu+1)}$, $F_{\mathrm{Sq}} = -\mu^2/(\nu+1)$.
3. Rectangles: $a_3 = a_4 = 0$ and $a_1 = a_2 = \sqrt{\mu/(\gamma+1)}$, $F_{\mathrm{Rect}} = -\mu^2/(\gamma+1)$.
4. One-dimensional quasipattern: $a_4 = 0$ and

$$a_2 = \sqrt{\frac{\mu(1+\nu-2\gamma)}{1+\nu-2\gamma^2}}, \qquad a_1 = a_3 = \sqrt{\frac{\mu(1-\gamma)}{1+\nu-2\gamma^2}}, \tag{6}$$

$$\Rightarrow F_{\mathrm{1DQ}} = -\frac{\mu^2}{2}\frac{3+\nu-4\gamma}{1+\nu-2\gamma^2}. \tag{7}$$

   It is quasiperiodic in the direction of $\mathbf{k}_2$ and periodic along $\mathbf{k}_4$. As is typical for solutions with sub-maximal isotropy, this solution exists only over a limited range of the nonlinear coefficients $(1+\nu-2\gamma)(1-\gamma) > 0$. It is always unstable [2].
5. Quasipattern: $a_1 = \cdots = a_4 = R$, with R satisfying

$$R = \sqrt{\frac{\mu}{1+\nu+2\gamma}} \Rightarrow F_{\mathrm{Q}} = -\frac{2\mu^2}{1+\nu+2\gamma}. \tag{8}$$

The conditions for linear stability of these solutions are given by:

1. Rolls: $\nu > 1$, $\gamma > 1$.

2. Squares: $\gamma > \frac{1}{2}(1+\nu)$, $-1 < \nu < 1$.
3. Rectangles: $\nu > 1$, $-1 < \gamma < 1$.
4. Quasipattern: $-\frac{1}{2}(1+\nu) < \gamma < \frac{1}{2}(1+\nu)$, $-1 < \nu < 1$.

2.2. Long-wave analysis

We assume that the conditions for the two-dimensional quasipattern to be stable with respect to homogeneous perturbations are satisfied and study its stability to sideband perturbations. In particular, we study the stability of the pattern as a function of its wavenumber. We will restrict the analysis to perfect quasipatterns, in which the wavenumber is the same in all the modes. This will allow us to obtain analytical expressions for the stability boundaries. A perfect quasipattern with wavenumber $\mathbf{k}$ slightly different from critical is given by $A_i = R\,\mathrm{e}^{\mathrm{i}q\hat{\mathbf{n}}_i\cdot\mathbf{x}}$, with $R = |A_1| = |A_2| = |A_3| = |A_4| = \sqrt{(\mu - q^2)/(1+\nu+2\gamma)}$ and $\eta q = |\mathbf{k} - \mathbf{k}_c|$. We expand around this solution, $A_i = (R + r_i)\,\mathrm{e}^{\mathrm{i}(q\hat{\mathbf{n}}_i\cdot\mathbf{x}+\phi_i)}$. Considering first only homogeneous perturbations ($r_i = r_i(t)$, $\phi_i = \phi_i(t)$) and separating real and imaginary parts, the linearized equations for the perturbations are:

$$\partial_t r_i = -2R^2 r_i - 2\nu R^2 r_{i+2} - 2\gamma R^2 (r_{i+1} + r_{i+3}), \tag{9}$$

$$\partial_t \phi_i = 0. \tag{10}$$

For the amplitude perturbations there are three eigenvalues, two corresponding to one-dimensional eigenspaces, $\sigma_{\hat{r}_1} = -2R^2(1+\nu+2\gamma)$ for $v_{\hat{r}_1} = \frac{1}{2}[r_1 = 1, r_2 = 1, r_3 = 1, r_4 = 1]$, and $\sigma_{\hat{r}_2} = -2R^2(1+\nu-2\gamma)$ for $v_{\hat{r}_2} = \frac{1}{2}[-1, 1, -1, 1]$. The other eigenvalue $\sigma_{\hat{r}_3,\hat{r}_4} = -2R^2(1-\nu)$ corresponds to a two-dimensional eigenspace spanned by $v_{\hat{r}_3} = \frac{1}{2}[-1, -1, 1, 1]$, $v_{\hat{r}_4} = \frac{1}{2}[-1, 1, 1, -1]$.

The four phases are marginal modes. Physically, it is more convenient to rearrange them into phase and phason modes. The first two are related to translations in space and can be written as

$$u^{\mathrm{T}}_{\phi_x} = \left[\phi_1 = \frac{1}{\sqrt{2}}, \phi_2 = \frac{1}{\sqrt{2}}\cos\left(\frac{2\pi}{8}\right), \phi_3 = 0, \phi_4 = \frac{1}{\sqrt{2}}\cos\left(\frac{6\pi}{8}\right)\right], \tag{11}$$

$$u^{\mathrm{T}}_{\phi_y} = \frac{1}{\sqrt{2}}\left[0,\ \sin\left(\frac{2\pi}{8}\right),\ \sin\left(\frac{4\pi}{8}\right),\ \sin\left(\frac{6\pi}{8}\right)\right]. \tag{12}$$

There still remains a two-dimensional subspace orthogonal to this one. An orthonormal basis for it is given by

$$u^{\mathrm{T}}_{\varphi_1} = \frac{1}{\sqrt{2}}\left[1, -\cos\left(\frac{2\pi}{8}\right),\ \cos\left(\frac{4\pi}{8}\right), -\cos\left(\frac{6\pi}{8}\right)\right], \tag{13}$$

$$u^{\mathrm{T}}_{\varphi_2} = \frac{1}{\sqrt{2}}\left[0, -\sin\left(\frac{2\pi}{8}\right),\ \sin\left(\frac{4\pi}{8}\right), -\sin\left(\frac{6\pi}{8}\right)\right]. \tag{14}$$

This choice of the phason modes corresponds to relative translations (in the x- and y-directions, respectively) between the two square lattices that compose the quasipattern. It is worth mentioning that the phason modes do not transform as a vector. In fact, under rotations by an angle θ, the transformation of the phason field $\tilde{\varphi} = (\varphi_1, \varphi_2)$ corresponds to that of a regular vector for a rotation by an angle 5θ (cf. Eqs. (30), (31)).

When spatial modulations are included, the perturbation equations become

$$\partial_t r_i = -2qR(\hat{\mathbf{n}}_i\cdot\nabla)\phi_i + (\hat{\mathbf{n}}_i\cdot\nabla)^2 r_i - 2R^2 r_i - 2\nu R^2 r_{i+2} - 2\gamma R^2(r_{i+1} + r_{i+3}), \tag{15}$$

$$\partial_t \phi_i = (\hat{\mathbf{n}}_i\cdot\nabla)^2\phi_i + \frac{2q}{R}(\hat{\mathbf{n}}_i\cdot\nabla)r_i. \tag{16}$$

Now the phase modes are no longer marginal, but exhibit diffusive dynamics. In order to study these long-wave dynamics, we define a small parameter ϵ and introduce slow time and space scales: ϵt, $\epsilon^{1/2}\mathbf{x}$. The amplitude and phase perturbations are expanded as

$$r_i(\epsilon^{1/2}\mathbf{x}, \epsilon t) = \epsilon \sum_{j=1}^{4} \hat{r}_j^i(\epsilon^{1/2}\mathbf{x}, \epsilon t) v_{\hat{r}_j}^i, \tag{17}$$

$$\phi_i(\epsilon^{1/2}\mathbf{x}, \epsilon t) = \epsilon^{1/2}[\phi_x(\epsilon^{1/2}\mathbf{x}, \epsilon t)u_{\phi_x}^i + \phi_y(\epsilon^{1/2}\mathbf{x}, \epsilon t)u_{\phi_y}^i + \varphi_1(\epsilon^{1/2}\mathbf{x}, \epsilon t)u_{\varphi_1}^i + \varphi_2(\epsilon^{1/2}\mathbf{x}, \epsilon t)u_{\varphi_2}^i]. \tag{18}$$

Inserting the expansion into Eqs. (15) and (16), we obtain at order $\epsilon^{1/2}$ the eigenvalues for the homogeneous perturbations, at order ϵ a relation between the stable and marginal modes of the type $\hat{r}_i = f_i(\nabla\phi_x, \nabla\phi_y, \nabla\varphi_1, \nabla\varphi_2)$, and at order $\epsilon^{3/2}$ a solvability condition for the marginal modes. This gives us the slow, long-wave dynamics. In component form the final equations are

$$\partial_t\phi_x = D_1\nabla^2\phi_x + (D_2 - D_1)\partial_x(\nabla\cdot\vec{\phi}) + D_3(\partial_x^2\varphi_1 - 2\partial_{xy}^2\varphi_2 - \partial_y^2\varphi_1), \tag{19}$$

$$\partial_t\phi_y = D_1\nabla^2\phi_y + (D_2 - D_1)\partial_y(\nabla\cdot\vec{\phi}) + D_3(-\partial_x^2\varphi_2 - 2\partial_{xy}^2\varphi_1 + \partial_y^2\varphi_2), \tag{20}$$

$$\partial_t\varphi_1 = D_4\nabla^2\varphi_1 + (D_5 - D_4)\partial_x(\partial_x\varphi_1 + \partial_y\varphi_2) + D_3(\partial_x^2\phi_x - 2\partial_{xy}^2\phi_y - \partial_y^2\phi_x), \tag{21}$$

$$\partial_t\varphi_2 = D_4\nabla^2\varphi_2 + (D_5 - D_4)\partial_y(\partial_x\varphi_1 + \partial_y\varphi_2) + D_3(-\partial_x^2\phi_y - 2\partial_{xy}^2\phi_x + \partial_y^2\phi_y), \tag{22}$$

where the values of the coefficients are given by

$$D_1 = \frac{1}{4} - \frac{q^2}{u}, \tag{23}$$

$$D_2 = \frac{3}{4} - \frac{q^2}{u} - \frac{2q^2}{v_1} = D_1 + D_2', \tag{24}$$

$$D_3 = D_1, \tag{25}$$

$$D_4 = D_1, \tag{26}$$

$$D_5 = \frac{3}{4} - \frac{q^2}{u} - \frac{2q^2}{v_2} = D_1 + D_5' \tag{27}$$

with $v_1 = 2R^2(1 + \nu + 2\gamma)$, $v_2 = 2R^2(1 + \nu - 2\gamma)$, $u = 2R^2(1 - \nu)$, and R given by Eq. (8) with μ replaced by $\mu - q^2$. Eqs. (19)–(22) are the diffusive analog of the elastic equations for octagonal quasicrystals, and their form can be deduced directly by means of symmetry arguments (see, for instance [24], in the case of quasicrystals).

A more compact notation, in which the symmetries become more evident, can be achieved by writing the phase and phason modes as complex fields. Let $\phi = \phi_x + \mathrm{i}\phi_y$, $\varphi = \varphi_1 + \mathrm{i}\varphi_2$ and $\nabla = \partial_X + \mathrm{i}\partial_Y$. Then the former expressions become

$$\partial_t\phi = D_1|\nabla|^2\phi + \tfrac{1}{2}(D_2 - D_1)\nabla(\bar{\nabla}\phi + \nabla\bar{\phi}) + D_3\,\mathrm{e}^{\mathrm{i}\xi}\bar{\nabla}^2\bar{\varphi}, \tag{28}$$

$$\partial_t\varphi = D_4|\nabla|^2\varphi + \tfrac{1}{2}(D_5 - D_4)\nabla(\bar{\nabla}\varphi + \nabla\bar{\varphi}) + D_3\,\mathrm{e}^{\mathrm{i}\xi}\bar{\nabla}^2\bar{\phi}. \tag{29}$$

The angle ξ depends on the basis that is chosen for the phase and phason modes. Since the specific choice does not have any physical relevance, α does not appear in the dispersion relation. In our case, $\xi = 0$. Now it is easy to see that these equations are invariant under rotations of $n\pi/4$. In fact, under such a rotation $\phi \to \mathrm{e}^{n\pi\mathrm{i}/4}\phi$, $\nabla \to \mathrm{e}^{n\pi\mathrm{i}/4}\nabla$,

$\varphi \to \mathrm{e}^{5n\pi \mathrm{i}/4}\varphi$, and consequently

$$\bar{\nabla}^2\bar{\phi} \to \mathrm{e}^{-2n\pi \mathrm{i}/4}\bar{\nabla}^2\,\mathrm{e}^{-n\pi \mathrm{i}/4}\bar{\phi} = \mathrm{e}^{-3n\pi \mathrm{i}/4}\bar{\nabla}^2\bar{\phi}, \tag{30}$$

$$\bar{\nabla}^2\bar{\varphi} \to \mathrm{e}^{-2n\pi \mathrm{i}/4}\bar{\nabla}^2\,\mathrm{e}^{-5n\pi \mathrm{i}/4}\bar{\varphi} = \mathrm{e}^{n\pi \mathrm{i}/4}\bar{\nabla}^2\bar{\varphi}. \tag{31}$$

Thus, while $\bar{\nabla}^2\bar{\phi}$ transforms as φ, $\bar{\nabla}^2\bar{\varphi}$ transforms as ϕ.

In order to calculate the stability boundaries, normal modes must be considered: $\phi = \phi_0\,\mathrm{e}^{\mathrm{i}\mathbf{Q}\cdot\mathbf{x}}$, $\varphi = \varphi_0\,\mathrm{e}^{\mathrm{i}\mathbf{Q}\cdot\mathbf{x}}$. From Eqs. (19)–(22), it can be shown that the stability curves are given by the expression:

$$2D_1D_2D_4D_5 = D_3^2[(D_1+D_2)(D_4+D_5) + (D_1-D_2)(D_4-D_5)\cos(8\theta) - 2D_3^2], \tag{32}$$

or, using Eqs. (23)–(27):

$$D_1^2D_2'D_5'\sin^2(4\theta) = 0, \tag{33}$$

where $\theta = \arctan(Q_y/Q_x)$. When $\theta = n\pi/4$, this condition is always satisfied. In this case, the eigenvalues are

$$\sigma_1 = 0, \qquad \sigma_2 = -2D_1Q^2, \tag{34}$$

$$\sigma_{3,4} = \frac{1}{2}\left(-2D_1 - D_2' - D_5' \pm \sqrt{4D_1^2 + (D_2'-D_5')^2}\right)Q^2, \tag{35}$$

and one of the eigenvalues is always marginal. (From Eqs. (15) and (16), it is easy to see that the growth rate of a perturbation to the phase ϕ_i in a direction perpendicular to $\hat{\mathbf{n}}_i$ is zero.) This means that the perturbations perpendicular to each set of rolls evolve on a still slower time scale that is not captured with Eq. (1). This situation is equivalent to that of the zig-zag instability of rolls or squares [25,26], and we will consider it separately.

When $\theta \neq n\pi/4$, the expression for the eigenvalues becomes very complicated, but the stability limits are given by the condition $D_1^2D_2'D_5' = 0$. Thus, two eigenvalues become zero when $D_1 = 0$ and the other two when $D_2' = 0$ and $D_5' = 0$, respectively. From this, the stability curves are given by

$$D_1 = 0 \Rightarrow \mu_1 = \frac{3+\nu+4\gamma}{1-\nu}q^2, \tag{36}$$

$$D_2' = 0 \Rightarrow \mu_2 = 3q^2, \tag{37}$$

$$D_5' = 0 \Rightarrow \mu_5 = \frac{3+3\nu+2\gamma}{1+\nu-2\gamma}q^2. \tag{38}$$

When $\gamma = 0$, the former equations reduce to the long-wave stability limits found in the case of square patterns [26]. It is interesting to note that the instability corresponding to $D_2' = 0$ is given by the usual value for the Eckhaus curve. Typical stability diagrams are shown in Fig. 3. When $\nu = \gamma$, the problem is degenerate and $\mu_1 = \mu_5$ (Fig. 3a). Which instability occurs first depends on the values of the coefficients ν and γ. For $\gamma > 0, \nu < \gamma$; $\nu+\gamma < 0, \gamma < 0$; and $\nu+\gamma > 0, \nu > \gamma$, the first instability is that corresponding to D_5', D_2', and D_1, respectively. The third case is shown in Fig. 3b. The symbols denote the results obtained linearizing Eq. (1) and solving the eigenvalue problem associated with the 8×8 matrix. These results agree perfectly with those obtained with the long-wave approximation, showing that the relevant instabilities are long wave.

The stability of the zig-zag mode cannot be studied within Eq. (1). In order to resolve the degeneracy when $\theta = n\pi/4$, it is necessary to go to higher order in the gradient expansion, to include derivative terms in the direction perpendicular to each set of rolls. Then, in Eq. (1), we use the replacement

$$(\hat{\mathbf{n}}_i\cdot\nabla)^2 \to [(\hat{\mathbf{n}}_i\cdot\nabla) - \mathrm{i}\delta\nabla^2]^2, \tag{39}$$

where δ is a small coefficient, whose size depends on the distance from threshold, $\delta = \mathrm{O}(\eta)$.

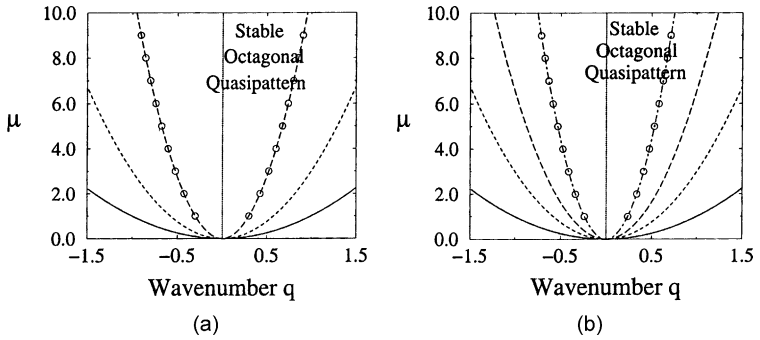

Fig. 3. Stability diagrams for: (a) $\nu = \gamma = 0.5$, and (b) $\nu = 0.7$, $\gamma = 0.4$. The short-dashed, dashed and dot-dashed lines correspond to $D_2' = 0$, $D_5' = 0$ and $D_1 = 0$, respectively. In (a) and (b), the dotted line gives the zig-zag instability. The circles are obtained solving the full dispersion relation associated with Eqs. (15) and (16).

This is equivalent to the Newell–Whitehead–Segel operator (NWS) $(\partial_x + \mathrm{i}\partial_y^2/k_c)^2$ in the case of rolls. However, the intrinsic anisotropy of the rolls makes the modulations in the x- and y-directions scale differently, so the ∂_x and ∂_y^2 terms in the NWS operator appear at the same order in the perturbation expansion. In our case, on the other hand, this distinction between normal and perpendicular directions is no longer possible, and the term ∇^2 is formally of higher order. As a result, the zig-zag instability evolves in a much longer time scale than the rest of the instabilities.

On this time scale, the perturbations associated with the other instabilities will decay, and we can assume that the phase of each of the modes only depends on the direction perpendicular to that mode. Then it is easy to see that the equations decouple. On a super-slow time, $\epsilon^4 t$, and taking q to be small, $q = \epsilon^2 \tilde{q}$, the usual nonlinear phase equation for the zig-zag instability is obtained

$$\partial_t \phi_i = 2\tilde{q}\delta(\hat{\tau}_i \cdot \nabla)^2 \phi_i - \delta^2(\hat{\tau}_i \cdot \nabla)^4 \phi_i + 6\delta^2[(\hat{\tau}_i \cdot \nabla)\phi_i]^2(\hat{\tau}_i \cdot \nabla)^2 \phi_i, \tag{40}$$

where $\hat{\tau}_i$ is the unit vector perpendicular to $\hat{\mathbf{n}}_i$. When $\tilde{q} < 0$, the pattern is unstable. As the coefficient in front of the cubic term is positive, the instability is supercritical. In order to confirm this, we have performed numerical simulations of the amplitude equations (1) using a fourth-order Runge–Kutta method with an integrating factor that computes the linear derivative terms exactly in Fourier space. In Fig. 4, the evolution of this zig-zag instability is shown, starting with a perturbation of the quasipattern in the direction perpendicular to

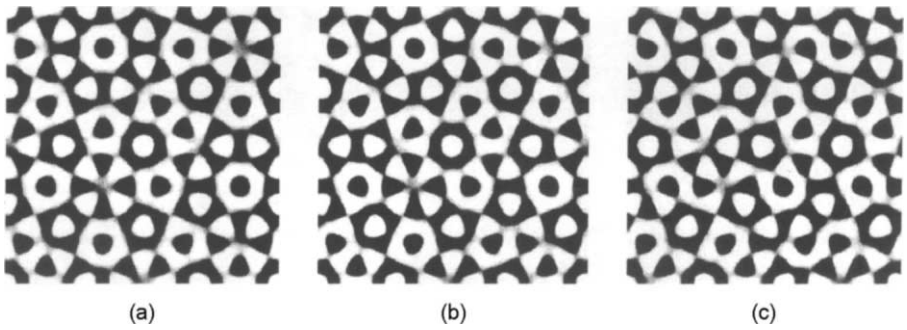

Fig. 4. Reconstruction of the octagonal quasipattern from the amplitudes A_i for the zig-zag instability at the times: (a) $t = 0$, (b) $t = 1000$, and (c) $t = 3000$. The simulations are done with 64×64 Fourier modes and the values of the coefficients: $\mu = 5$, $\nu = 0.7$, $\gamma = 0.4$, $q = -0.05$, $L = 25$, $k_c = 10k_{\min}$ and $\delta = 0.1$.

$\hat{\mathbf{n}}_i$: $A_1 = R\,\mathrm{e}^{\mathrm{i}qx}(1 + 0.1\mathrm{i}\cos(4\pi y/L))$, $A_j = R\,\mathrm{e}^{\mathrm{i}q\hat{\mathbf{n}}_i\cdot\mathbf{x}}$, $j \neq 1$. As expected, the instability saturates, resulting in a distorted quasipattern.

3. Decagonal quasipatterns

3.1. Ginzburg–Landau equations

For the decagonal quasipattern, we consider the expansion (cf. Fig. 1b), $\psi = \eta\sum_{n=1}^{5} A_n(\mathbf{x}, t)\,\mathrm{e}^{\mathrm{i}\mathbf{k}_n\cdot\mathbf{x}} + \text{c.c.} + \text{h.o.t.}$ The amplitudes $A_i(\mathbf{x}, t)$ now satisfy the equations

$$\partial_t A_i = \mu A_i + (\hat{\mathbf{n}}_i\cdot\nabla)^2 A_i - A_i[|A_i|^2 + \nu(|A_{i+1}|^2 + |A_{i+4}|^2) + \gamma(|A_{i+2}|^2 + |A_{i+3}|^2)] + \alpha\overline{A_{i+1}A_{i+2}A_{i+3}A_{i+4}}, \tag{41}$$

where μ is the control parameter and ν and γ measure the interaction between modes subtending an angle of $2\pi/5$ and $4\pi/5$, respectively. The indices are repeated cyclically with period 5. Although the quartic term is higher order than the others, we have included it in Eq. (41) to account for the resonant interaction among the five wavevectors, $\sum_{j=1}^{5}\hat{\mathbf{k}}_j = 0$ (see Fig. 1b). Without this term there would be a spurious one-parameter class of solutions, parameterized by the global phase, $\Phi = \sum_{j=1}^{5}\phi_j$, all with the same energy. The resonance term lifts this degeneracy by rendering the global phase (slightly) damped.

The Lyapunov functional for the decagonal case is given by

$$\mathcal{F} = \iint \mathrm{d}x\,\mathrm{d}y \sum_{i=1}^{5}[-\mu|A_i|^2 + |(\hat{\mathbf{n}}_i\cdot\nabla)^2 A_i|^2 + \tfrac{1}{2}|A_i|^4 + \nu|A_i|^2|A_{i+1}|^2 + \gamma|A_i|^2|A_{i+2}|^2] - \alpha(A_1A_2A_3A_4A_5 + \text{c.c.}). \tag{42}$$

Writing again $A_j = a_j\,\mathrm{e}^{\mathrm{i}\phi_j}$, we now have

$$\partial_t a_i = \mu a_i - a_i[a_i^2 + \nu(a_{i+1}^2 + a_{i+4}^2) + \gamma(a_{i+2}^2 + a_{i+3}^2)] + \alpha a_{i+1}a_{i+2}a_{i+3}a_{i+4}\cos(\Phi), \tag{43}$$

$$a_i\,\partial_t\phi_i = -\alpha a_{i+1}a_{i+2}a_{i+3}a_{i+4}\sin(\Phi) \tag{44}$$

with $\Phi = \sum_{j=1}^{5}\phi_j$, the global phase. For a quasiperiodic solution, $a_1 = \cdots = a_5 = R$ and Eq. (44) becomes

$$\partial_t\Phi = -5\alpha R^3\sin(\Phi). \tag{45}$$

There are two stationary solutions: one stable ($\Phi = 0$), the other unstable ($\Phi = \pi$). We will consider the former one.

Because the resonant term involving α is quartic, it cannot appear in systems with the reflection symmetry $A_i \to -A_i$ which arises, for instance, in Boussinesq convection or in Faraday waves with one-frequency forcing. In that case ($\alpha = 0$), Φ is arbitrary to the order considered in Eq. (41) and, for $\Phi \neq 0, \pi$, solutions with pentagonal rather than decagonal symmetry can bifurcate from the trivial state. The situation is analogous to that of the triangle solutions in the case of hexagonal symmetry [27]. The global phase gets fixed by the higher-order resonance term $\bar{A}_i|A_{i+1}|^2|A_{i+2}|^2|A_{i+3}|^2|A_{i+4}|^2$, which leads to $\partial_t\Phi \sim \sin(2\Phi)$, implying $\Phi = n\pi/2$ for the regular pentagonal solution. We will not consider these solutions in the following and take $\phi_1 = \cdots = \phi_5 = 0$.

There are six different kinds of simple solutions (see Fig. 5): rolls, two types of rectangles, two types of one-dimensional quasipatterns and the decagonal quasipattern. They are given by:

1. Rolls: $a_2 = \cdots = a_5 = 0$ and $a_1 = \sqrt{\mu}$, $F_{\mathrm{R}} = -\frac{1}{2}\mu^2$.

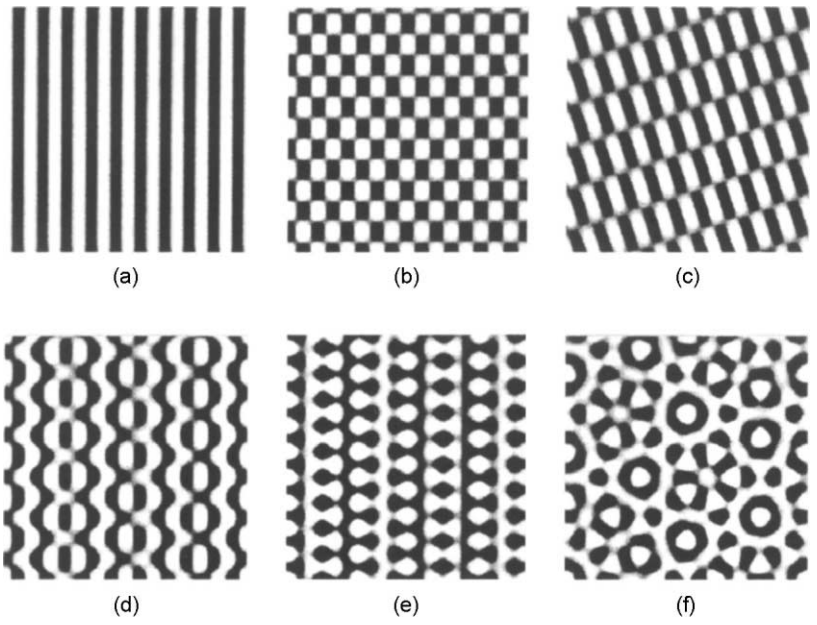

Fig. 5. Decagonal case. Different types of solutions of Eq. (41): (a) rolls, (b) rectangles (R_1), (c) rectangles (R_2), (d) and (e) 1D quasipatterns (H_1) and (H_2), and (f) decagonal quasipattern.

2. Rectangles (R_1): $a_1 = a_2 = a_5 = 0$ and $a_3 = a_4 = \sqrt{\mu/(\nu+1)}$, $F_{R_1} = -\mu^2/(\nu+1)$.
3. Rectangles (R_2): $a_2 = a_3 = a_5 = 0$ and $a_1 = a_4 = \sqrt{\mu/(\gamma+1)}$, $F_{R_2} = -\mu^2/(\gamma+1)$.
4. One-dimensional quasipatterns (H_1): $a_2 = a_5 = 0$ and

$$a_1 = \sqrt{\frac{\mu(1+\nu-2\gamma)}{1+\nu-2\gamma^2}}, \qquad a_3 = a_4 = \sqrt{\frac{\mu(1-\gamma)}{1+\nu-2\gamma^2}}, \tag{46}$$

$$F_{H_1} = -\frac{\mu^2}{2}\frac{\nu+3-4\gamma}{\nu-2\gamma^2+1}. \tag{47}$$

They exist provided $(1-\gamma)(1+\nu-2\gamma) > 0$.

5. One-dimensional quasipatterns (H_2): $a_3 = a_4 = 0$ and

$$a_1 = \sqrt{\frac{\mu(1+\gamma-2\nu)}{1+\gamma-2\nu^2}}, \qquad a_2 = a_5 = \sqrt{\frac{\mu(1-\nu)}{1+\gamma-2\nu^2}}, \tag{48}$$

$$F_{H_2} = -\frac{\mu^2}{2}\frac{3+\gamma-4\nu}{1+\gamma-2\nu^2}. \tag{49}$$

They exist provided $(1-\nu)(1+\gamma-2\nu) > 0$. Both H_1 and H_2 are quasiperiodic in one dimension and periodic in the other.

6. Quasipattern: $a_1 = \cdots = a_5 = R$, with R satisfying

$$0 = \mu - (1+2\nu+2\gamma)R^2 + \alpha R^3. \tag{50}$$

The analytic solution is quite complicated. For $\alpha = 0$, it simplifies to

$$R = \sqrt{\frac{\mu}{1+2\nu+2\gamma}} \Rightarrow F_{\mathrm{Q}} = -\frac{5}{2}\frac{\mu^2}{1+2\nu+2\gamma}. \tag{51}$$

7. In addition, when $\alpha = 0$, there is another solution, with $a_5 = 0$ and

$$a_1 = a_4 = \sqrt{\frac{\mu(1-\nu)}{1+\gamma+\nu+\gamma\nu-\nu^2-\gamma^2}}, \tag{52}$$

$$a_2 = a_3 = \sqrt{\frac{\mu(1-\gamma)}{1+\gamma+\nu+\gamma\nu-\nu^2-\gamma^2}}. \tag{53}$$

It is also quasiperiodic in the two spatial dimensions and exists if $(1-\nu)(1-\gamma) > 0$.

The conditions for linear stability are:

1. Rolls: $\nu > 1, \gamma > 1$.
2. Rectangles (R_1): $-1 < \nu < 1, \gamma > 1$.
3. Rectangles (R_2): $\nu > 1, -1 < \gamma < 1$.
4. 1D quasipattern (H_1):

$$2\gamma - 1 < \nu < 1, \tag{54}$$

$$1 - \nu\tfrac{1}{2}(1+\sqrt{5}) - \gamma\tfrac{1}{2}(1-\sqrt{5}) < 0. \tag{55}$$

5. 1D quasipattern (H_2):

$$2\nu - 1 < \gamma < 1, \tag{56}$$

$$1 - \nu\tfrac{1}{2}(1-\sqrt{5}) - \gamma\tfrac{1}{2}(1+\sqrt{5}) < 0. \tag{57}$$

6. The quasiperiodic solution given by Eqs. (52) and (53) is always unstable.
7. Decagonal quasipattern:

$$1 - \nu\tfrac{1}{2}(1+\sqrt{5}) - \gamma\tfrac{1}{2}(1-\sqrt{5}) + R\alpha > 0, \tag{58}$$

$$1 - \nu\tfrac{1}{2}(1-\sqrt{5}) - \gamma\tfrac{1}{2}(1+\sqrt{5}) + R\alpha > 0, \tag{59}$$

$$2(1+2\nu+2\gamma) - 3\alpha R > 0. \tag{60}$$

When (60) is violated, the quasipattern undergoes a saddle-node bifurcation that generates an unstable branch with larger amplitude (see Fig. 6). For these amplitudes, the quartic term is of the same order as the other terms in Eq. (41), which is inconsistent with the amplitude expansion. We restrict ourselves therefore to the range $3\alpha R \ll 2(1+2\nu+2\gamma)$.

For $R = 0$, Eqs. (58) and (59) are complementary to the stability conditions (55) and (57) for the one-dimensional quasipatterns. Thus, at onset one of the one-dimensional quasipatterns can be stable, while the two-dimensional quasipattern is unstable (or vice versa). For $\alpha > 0$, the two-dimensional quasipattern can gain stability with increasing μ, while the one-dimensional quasipattern is still stable. This bistability is expected to persist even if higher-order terms were included in the Ginzburg–Landau equations (41), since they would contribute only terms of the order R^2 to the stability conditions. For a small range of parameters ν and γ, the stabilization of the two-dimensional quasipattern can occur for amplitudes for which these higher-order terms would still be negligible.

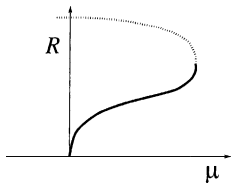

Fig. 6. Sketch of the bifurcation diagram for the decagonal quasipattern, as given by Eq. (50) (solid and dotted lines representing stable and unstable branches, respectively). The saddle-node bifurcation occurs at amplitudes for which (41) is not valid any more.

3.2. Long-wave analysis

Proceeding as in the case of the octagonal quasipattern, we obtain for the linearized perturbation equations

$$\partial_t r_i = -2qR(\hat{\mathbf{n}}_i\cdot\nabla)\phi_i + (\hat{\mathbf{n}}_i\cdot\nabla)^2 r_i + R^3\alpha\left(\sum_{j=1}^{5} r_j - 2r_i\right) - 2R^2 r_i$$
$$-2\nu R^2(r_{i+1}+r_{i-1}) - 2\gamma R^2(r_{i+2}+r_{i-2}), \tag{61}$$

$$\partial_t \phi_i = (\hat{\mathbf{n}}_i\cdot\nabla)^2\phi_i + \frac{2q}{R}(\hat{\mathbf{n}}_i\cdot\nabla)r_i - \alpha R^3\sum_{j=1}^{5}\phi_j \tag{62}$$

with R satisfying

$$0 = (\mu - q^2) - (1 + 2\nu + 2\gamma)R^2 + \alpha R^3. \tag{63}$$

For the amplitude perturbations there are three eigenvalues. One eigenvalue, $\sigma_{\mathrm{R}} = R^2(3\alpha R - 2 - 4\nu - 4\gamma)$, corresponds to a one-dimensional eigenspace spanned by

$$v_H^{\mathrm{T}} = \frac{1}{\sqrt{5}}[r_1 = 1, r_2 = 1, r_3 = 1, r_4 = 1, r_5 = 1]. \tag{64}$$

The other two eigenvalues are given by $\sigma_{T_{2,3}} = R^2(-2 - 2\alpha R + \nu(1 \pm \sqrt{5}) + \gamma(1 \mp \sqrt{5}))$ and each corresponds to 2 two-dimensional eigenspaces. Four orthonormal vectors spanning these spaces are

$$v_{T_1}^{\mathrm{T}} = \frac{1}{\sqrt{5+\sqrt{5}}}\left[-\frac{1+\sqrt{5}}{2}, \frac{1+\sqrt{5}}{2}, -1, 0, 1\right], \tag{65}$$

$$v_{T_3}^{\mathrm{T}} = \sqrt{\tfrac{1}{40}}[-(1-\sqrt{5}), -(1-\sqrt{5}), -(1+\sqrt{5}), 4, -(1+\sqrt{5})], \tag{66}$$

corresponding to σ_{T_2} and

$$v_{T_2}^{\mathrm{T}} = \frac{1}{\sqrt{5-\sqrt{5}}}\left[-1, \frac{1-\sqrt{5}}{2}, -\frac{1-\sqrt{5}}{2}, 1, 0\right], \tag{67}$$

$$v_{T_4}^{\mathrm{T}} = \sqrt{\tfrac{1}{40}}[-(1-\sqrt{5}), -(1+\sqrt{5}), -(1+\sqrt{5}), -(1-\sqrt{5}), 4] \tag{68}$$

to σ_{T_3}.

The global phase is a stable mode with a one-dimensional subspace spanned by $u_{\Phi}^{\mathrm{T}} = [\phi_1 = 1, \ldots, \phi_5 = 1]/\sqrt{5}$. As with the octagonal quasipattern, there are four marginal phase modes. The two corresponding to translations in space can be written as

$$u_{\phi_x}^{\mathrm{T}} = \sqrt{\frac{2}{5}}\left[1,\ \cos\left(\frac{2\pi}{5}\right),\ \cos\left(\frac{4\pi}{5}\right),\ \cos\left(\frac{6\pi}{5}\right),\ \cos\left(\frac{8\pi}{5}\right)\right], \tag{69}$$

$$u_{\phi_y}^{\mathrm{T}} = \sqrt{\frac{2}{5}}\left[0,\ \sin\left(\frac{2\pi}{5}\right),\ \sin\left(\frac{4\pi}{5}\right),\ \sin\left(\frac{6\pi}{5}\right),\ \sin\left(\frac{8\pi}{5}\right)\right]. \tag{70}$$

The two phason modes can be written as

$$u_{\varphi_1}^{\mathrm{T}} = \sqrt{\frac{2}{5}}\left[1,\ \cos\left(\frac{6\pi}{5}\right),\ \cos\left(\frac{12\pi}{5}\right),\ \cos\left(\frac{18\pi}{5}\right),\ \cos\left(\frac{24\pi}{5}\right)\right], \tag{71}$$

$$u_{\varphi_2}^{\mathrm{T}} = \sqrt{\frac{2}{5}}\left[0,\ \sin\left(\frac{6\pi}{5}\right),\ \sin\left(\frac{12\pi}{5}\right),\ \sin\left(\frac{18\pi}{5}\right),\ \sin\left(\frac{24\pi}{5}\right)\right]. \tag{72}$$

Under rotations, the phason mode $\tilde{\varphi} = (\varphi_1, \varphi_2)$ changes with twice the rotation angle.

The expansion of the perturbations includes now the global phase:

$$r_i(\mathbf{x}, t) = \epsilon \sum_{j=1}^{4} \hat{r}_j^i(\epsilon^{1/2}\mathbf{x}, \epsilon t) v_{\hat{r}_j}^i, \tag{73}$$

$$\begin{aligned}\phi_i(\mathbf{x}, t) = {} & \epsilon^{1/2}[\phi_x(\epsilon^{1/2}\mathbf{x}, \epsilon t)u_{\phi_x}^i + \phi_y(\epsilon^{1/2}\mathbf{x}, \epsilon t)u_{\phi_y}^i + \varphi_1(\epsilon^{1/2}\mathbf{x}, \epsilon t)u_{\varphi_1}^i + \varphi_2(\epsilon^{1/2}\mathbf{x}, \epsilon t)u_{\varphi_2}^i] \\ & + \epsilon\Phi(\epsilon^{1/2}\mathbf{x}, \epsilon t)u_{\Phi}^i,\end{aligned} \tag{74}$$

and the long-wave equations can be written as

$$\partial_t \phi_x = D_1\nabla^2\phi_x + D_2\partial_x(\nabla\cdot\vec{\phi}) + D_3(\partial_{x^2}^2\varphi_1 + 2\partial_{xy}^2\varphi_2 - \partial_{y^2}^2\varphi_1), \tag{75}$$

$$\partial_t \phi_y = D_1\nabla^2\phi_y + D_2\partial_y(\nabla\cdot\vec{\phi}) + D_3(\partial_{x^2}^2\varphi_1 - 2\partial_{xy}^2\varphi_1 - \partial_{y^2}^2\varphi_2), \tag{76}$$

$$\partial_t \varphi_1 = D_4\nabla^2\varphi_1 + D_3(\partial_{x^2}^2\phi_x - 2\partial_{xy}^2\phi_y - \partial_{y^2}^2\phi_x), \tag{77}$$

$$\partial_t \varphi_2 = D_4\nabla^2\varphi_2 + D_3(\partial_{x^2}^2\phi_y + 2\partial_{xy}^2\phi_x - \partial_{y^2}^2\phi_y). \tag{78}$$

The values of the coefficients are given by

$$D_1 = \frac{1}{4} - \frac{q^2}{u_1}, \tag{79}$$

$$D_2 = \frac{1}{2} - \frac{2q^2}{v}, \tag{80}$$

$$D_3 = D_1, \tag{81}$$

$$D_4 = \frac{1}{2} - \frac{q^2}{u_1} - \frac{q^2}{u_2} = D_1 + \tilde{D}_4 \quad \text{with } \tilde{D}_4 = \frac{1}{4} - \frac{q^2}{u_2} \tag{82}$$

with $u_1 = R^2(2(R\alpha + 1) - \nu(1 + \sqrt{5}) - \gamma(1 - \sqrt{5}))$, $u_2 = R^2(2(R\alpha + 1) - \nu(1 - \sqrt{5}) - \gamma(1 + \sqrt{5}))$, $v = R^2(2(1 + 2\nu + 2\gamma) - 3R\alpha)$, and R a solution of Eq. (63).

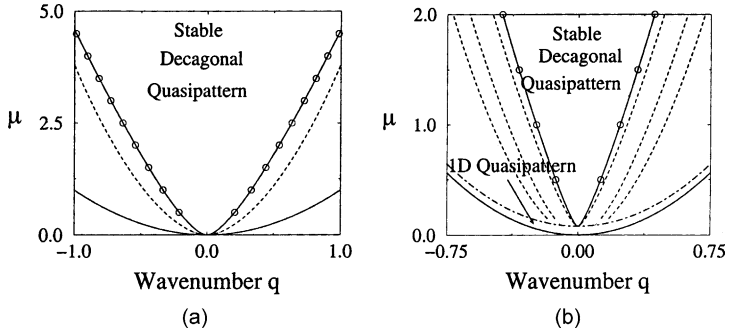

Fig. 7. Stability diagrams for $\alpha = 1$ and (a) $\nu = \gamma = 0.7$, and (b) $\nu = 0.5$, $\gamma = 0.9$. The dash-dotted line represents the line at which the 2D quasipattern becomes stable. Below this line, the 1D quasipattern H_2 is the only stable solution.

In complex form ($\phi = \phi_x + \mathrm{i}\phi_y$, $\varphi = \varphi_1 + \mathrm{i}\varphi_2$, $\nabla = \partial_x + \mathrm{i}\partial_y$), the phase equations read

$$\partial_t \phi = D_1|\nabla|^2\phi + \tfrac{1}{2}D_2\nabla(\bar{\nabla}\phi + \nabla\bar{\phi}) + D_3\,\mathrm{e}^{\mathrm{i}\xi}\bar{\nabla}^2\bar{\varphi}, \tag{83}$$

$$\partial_t \varphi = D_4|\nabla|^2\varphi + D_3\,\mathrm{e}^{\mathrm{i}\xi}\bar{\nabla}^2\bar{\phi}. \tag{84}$$

Again, the angle ξ depends on the relative orientation between the phase and phason modes. For the basis chosen, $\xi = 0$.

Considering normal modes, $\phi = \phi_0\,\mathrm{e}^{\mathrm{i}\mathbf{Q}\cdot\mathbf{x}}$, $\varphi = \varphi_0\,\mathrm{e}^{\mathrm{i}\mathbf{Q}\cdot\mathbf{x}}$, the eigenvalues now become

$$\sigma_{1,2} = -\frac{1}{2}\left[D_1 + D_4 \pm \sqrt{(D_1 - D_4)^2 + 4D_3^2}\right]Q^2, \tag{85}$$

$$\sigma_{3,4} = -\frac{1}{2}\left[D_1 + D_2 + D_4 \pm \sqrt{(D_1 + D_2 - D_4)^2 + 4D_3^2}\right]Q^2. \tag{86}$$

Typical stability diagrams are shown in Fig. 7. When $\nu = \gamma$, the eigenvalues become degenerate ($D_4 = 2D_1$ and three eigenvalues go through zero at the curve $u_1 = u_2 = 4q^2$). In Fig. 7b, the one-dimensional quasipattern persists amplitude-stable beyond the dash-dotted lines (cf. (57)). We have not investigated its stability with respect to sideband perturbations.

4. Dodecagonal quasipatterns

4.1. Ginzburg–Landau equations

Dodecagonal quasipatterns can be thought of as a combination of two rotated hexagon patterns. The amplitudes $A_i(\mathbf{x}, t)$ corresponding to the modes indicated in Fig. 1c satisfy the equations:

$$\begin{aligned}\partial_t A_i = {} & \mu A_i + (\hat{\mathbf{n}}_i \cdot \nabla)^2 A_i + \alpha\overline{A_{i+2}A_{i+4}} \\ & - A_i[|A_i|^2 + \nu(|A_{i+2}|^2 + |A_{i+4}|^2) + \gamma(|A_{i-1}|^2 + |A_{i-3}|^2) + 2\beta|A_{i+1}|^2], \quad i = 1, 3, 5,\end{aligned} \tag{87}$$

$$\begin{aligned}\partial_t A_i = {} & \mu A_i + (\hat{\mathbf{n}}_i \cdot \nabla)^2 A_i + \alpha\overline{A_{i+2}A_{i+4}} \\ & - A_i[|A_i|^2 + \nu(|A_{i+2}|^2 + |A_{i+4}|^2) + \gamma(|A_{i+1}|^2 + |A_{i+3}|^2) + 2\beta|A_{i-1}|^2], \quad i = 2, 4, 6.\end{aligned} \tag{88}$$

Here the indices are cyclic with period 6, μ is the control parameter and ν, γ, and β measure the interaction between modes subtending angles of $2\pi/3$, $\pi/6$ and $\pi/2$, respectively. The two hexagonal sub-lattices imply two resonance conditions: $\mathbf{k}_1+\mathbf{k}_3+\mathbf{k}_5=0$ and $\mathbf{k}_2+\mathbf{k}_4+\mathbf{k}_6=0$. Correspondingly, there are two global phases: $\Phi_1=\phi_1+\phi_3+\phi_5$ and $\Phi_2=\phi_2+\phi_4+\phi_6$.

The Lyapunov functional can be written as

$$\mathcal{F}=\iint \mathrm{d}x\,\mathrm{d}y \sum_{i=1}^{6}\left[-\mu|A_i|^2+|(\hat{\mathbf{n}}_i\cdot\nabla)^2A_i|^2+\frac{1}{2}|A_i|^4+\nu|A_i|^2|A_{i+2}|^2+\frac{\gamma}{2}|A_i|^2|A_{i+3}|^2 +\frac{\gamma+2\beta}{2}|A_i|^2|A_{i+1}|^2+\frac{(-1)^{i+1}(\gamma-2\beta)}{2}|A_i|^2|A_{i-1}|^2\right]-\alpha(A_1A_3A_5+A_2A_4A_6+\text{c.c.}). \tag{89}$$

In terms of the magnitudes a_i and phases ϕ_i, Eqs. (87) and (88) can be written as

$$\partial_t a_i=\mu a_i+\alpha a_{i+2}a_{i+4}\cos(\Phi)-a_i[a_i^2+\nu(a_{i+2}^2+a_{i+4}^2)+\gamma(a_{i\pm1}^2+a_{i\pm3}^2)+2\beta|a_{i\pm1}|^2], \tag{90}$$

$$a_i\partial_t\phi_i=-\alpha a_{i+2}a_{i+4}\sin(\Phi), \tag{91}$$

where $\Phi=\Phi_1$ or $\Phi=\Phi_2$ for i odd and i even, respectively. For hexagonal or dodecagonal patterns in which the nonzero amplitudes are fixed, $a_i=R$, Eq. (91) becomes

$$\partial_t\Phi_{1,2}=-3\alpha R\sin(\Phi_{1,2}). \tag{92}$$

Among the four solutions $\Phi_{1,2}=0$ and $\Phi_{1,2}=\pi$ only the one with $\Phi_1=\Phi_2=0$ is stable. In the following, we assume the amplitudes A_j to be real and take $\phi_1=\cdots=\phi_6=0$. Now the simple solutions include rolls, rectangles, squares, hexagons, mixed modes, one-dimensional quasipatterns and the dodecagonal quasipattern (see Fig. 8). They are given by:

1. Rolls: $a_2=\cdots=a_6=0$ and $a_1=\sqrt{\mu}$, $F_{\mathrm{R}}=-\frac{1}{2}\mu^2$.
2. Rectangles (R): $a_2=\cdots=a_5=0$ and $a_1=a_6=\sqrt{\mu/(\gamma+1)}$, $F_{R_1}=-\mu^2/(\gamma+1)$.
3. Squares (S): $a_3=\cdots=a_6=0$ and $a_1=a_2=\sqrt{\mu/(2\beta+1)}$, $F_{R_2}=-\mu^2/(2\beta+1)$.
4. Hexagons (H): $a_2=a_4=a_6=0$ and

$$a_1=a_3=a_5=\frac{\alpha\pm\sqrt{\alpha^2+4\mu(1+2\nu)}}{2(1+2\nu)}, \tag{93}$$

$$F_H=-\tfrac{3}{2}R^2[2\mu-R^2(1+2\nu)]-\alpha R^3. \tag{94}$$

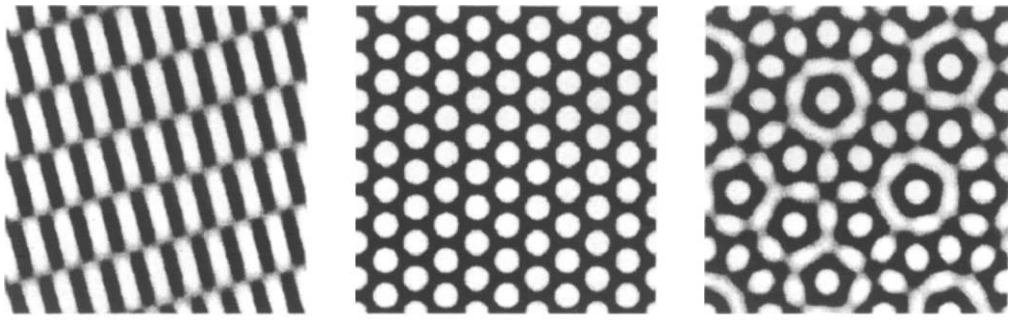

Fig. 8. Dodecagonal case. Several of the solutions of Eqs. (87) and (88): (a) rectangles, (b) hexagons, and (c) dodecagonal quasipattern.

5. Mixed mode: $a_2 = a_4 = a_6 = 0$, $a_1 = a_3 \neq a_5$. It is always unstable.
6. One-dimensional quasipattern: $a_2 = a_4 = 0$, $a_{1,3,5,6} \neq 0$.
7. Two-dimensional quasipattern: $a_1 = \cdots = a_6 = R$, with R given by

$$R = \frac{\alpha \pm \sqrt{\alpha^2 + 4\mu(1 + 2\nu + 2\gamma + 2\beta)}}{2(1 + 2\nu + 2\gamma + 2\beta)}, \tag{95}$$

$$F_Q = -3R^2[2\mu - R^2(1 + 2\nu + 2\gamma + 2\beta)] - 2\alpha R^3. \tag{96}$$

The relative stability of the former solutions is as follows:

1. Rolls are always unstable at onset. Provided $\nu > 1$, $\beta > \frac{1}{2}$ and $\gamma > 1$, they become stable at a larger value of μ, given by

$$\mu = \frac{\alpha^2}{(\nu - 1)^2}. \tag{97}$$

2. Rectangles are unstable at onset and become stable at

$$\mu = \frac{\alpha^2(1 + \gamma)}{(\nu - 1)(\nu + 2\beta - \gamma - 1)} \tag{98}$$

if $\nu > 1$ and $\nu + 2\beta > \gamma + 1 > 0$.
3. Squares are also unstable at onset. If $\nu + \gamma > 1 + 2\beta > 0$, they become stable at

$$\mu = \frac{\alpha^2(1 + 2\beta)}{(1 + 2\beta - \nu - \gamma)^2}. \tag{99}$$

4. Hexagons appear in a saddle-node bifurcation at

$$\mu = -\frac{\alpha^2}{4(1 + 2\nu)}, \tag{100}$$

but when $2(\gamma + \beta) < -(1 + 2\nu)$, they are always unstable with respect to the dodecagonal quasipattern. If $2(\gamma + \beta) > -(1 + 2\nu)$, they are stable at the saddle-node but can become unstable as a result of a secondary bifurcation. In particular, if $\nu > 1$, they can become unstable to rolls at

$$\mu = \frac{\alpha^2(2 + \nu)}{(\nu - 1)^2}, \tag{101}$$

and, when $1 + 2\nu > 2(\gamma + \beta)$, to the dodecagonal quasipattern for

$$\mu > \frac{2\alpha^2(\gamma + \beta)}{(1 + 2\nu - 2\gamma - 2\beta)^2}. \tag{102}$$

5. Dodecagonal quasipatterns appear in a saddle-node bifurcation at

$$\mu = -\frac{1}{4}\frac{\alpha^2}{(1 + 2\nu + 2\gamma + 2\beta)^2}. \tag{103}$$

When $2|\gamma + \beta| < 1 + 2\nu$, they are unstable at onset with respect to hexagons, but become stable through a secondary bifurcation, at

$$\mu = \frac{\alpha^2}{4}\frac{6\gamma + 6\beta - 2\nu - 1}{(1 + 2\nu - 2\gamma - 2\beta)^2}. \tag{104}$$

Therefore, there is hysteresis between hexagons and the dodecagonal quasipattern. A similar situation is found in the case of superlattices [23].

Besides, if $1+\gamma < \nu+2\beta$ or $1+2\beta < \gamma+\nu$, the quasipattern becomes again unstable to rectangles or squares, respectively. The values of the control parameter for these transitions are

$$\mu_{\mathrm{Rec}} = \frac{\alpha^2(3\gamma+\nu+2)}{(1+\gamma-\nu-2\beta)^2}, \tag{105}$$

$$\mu_{\mathrm{Sq}} = \frac{\alpha^2(2+\gamma+\nu+4\beta)}{(1+2\beta-\gamma-\nu)^2}. \tag{106}$$

4.2. Long-wave analysis

The long-wave analysis proceeds analogous to that of the previous cases. The linearized perturbation equations are given by

$$\begin{aligned}\partial_t r_i = {} & -2qR(\hat{\mathbf{n}}_i\cdot\nabla)\phi_i + (\hat{\mathbf{n}}_i\cdot\nabla)^2 r_i + R\alpha(r_{i+2}+r_{i+4}-r_i) - 2R^2 r_i - 2\nu R^2(r_{i+2}+r_{i+4}) \\ & -2\gamma R^2(r_{i\pm1}+r_{i\pm3}) - 4\beta R^2 r_{i\mp1},\end{aligned} \tag{107}$$

$$\partial_t\phi_i = (\hat{\mathbf{n}}_i\cdot\nabla)^2\phi_i + \frac{2q}{R}(\hat{\mathbf{n}}_i\cdot\nabla)r_i - \alpha R(\phi_i+\phi_{i+2}+\phi_{i+4}) \tag{108}$$

with

$$R = \frac{\alpha+\sqrt{\alpha^2+4(\mu-q^2)(1+2\nu+2\gamma+2\beta)}}{2(1+2\nu+2\gamma+2\beta)}. \tag{109}$$

For the amplitude perturbations there are four eigenvalues. Two correspond to one-dimensional eigenspaces, $\sigma_{T_1} = -R[2R(1+2\nu+2\gamma+2\beta)-\alpha]$, with eigenvector $v_H^{\mathrm{T}} = [1,1,1,1,1,1]/\sqrt{6}$ and $\sigma_{T_2} = -R[2R(1+2\nu-2\gamma-2\beta)-\alpha]$, with $v_{T_1} = [-1,1,-1,1,-1,1]/\sqrt{6}$. The other four eigenvalues $\sigma_{T_{3,4}} = -2R[R(1+\gamma-2\beta-\nu)+\alpha]$ and $\sigma_{T_{5,6}} = -2R[R(1+2\beta-\gamma-\nu)+\alpha]$ are associated with 2 two-dimensional eigenspaces. Four orthonormal vectors spanning these spaces are

$$v_{T_3}^{\mathrm{T}} = [-\tfrac{1}{2},\tfrac{1}{2},\tfrac{1}{2},-\tfrac{1}{2},0,0], \qquad v_{T_4}^{\mathrm{T}} = [-\tfrac{1}{2},\tfrac{1}{2},0,0,\tfrac{1}{2},-\tfrac{1}{2}], \tag{110}$$

corresponding to $\sigma_{T_{3,4}}$ and

$$v_{T_5}^{\mathrm{T}} = [\tfrac{1}{2},\tfrac{1}{2},0,0,-\tfrac{1}{2},-\tfrac{1}{2}], \qquad v_{T_6}^{\mathrm{T}} = [0,0,\tfrac{1}{2},\tfrac{1}{2},-\tfrac{1}{2},-\tfrac{1}{2}], \tag{111}$$

to $\sigma_{T_{4,5}}$.

The global phases are again stable modes with one-dimensional subspaces spanned by $u_{\Phi_1}^{\mathrm{T}} = [1,0,1,0,1,0]/\sqrt{3}$ and $u_{\Phi_2}^{\mathrm{T}} = [0,1,0,1,0,1]/\sqrt{3}$. There are four marginal modes. The two phase modes corresponding to translations in space can be written as

$$u_{\phi_x}^{\mathrm{T}} = \frac{[1,0,-\frac{1}{2},-\frac{1}{2}\sqrt{3},-\frac{1}{2},\frac{1}{2}\sqrt{3}]}{\sqrt{3}}, \tag{112}$$

$$u_{\phi_y}^{\mathrm{T}} = \frac{[0,1,\frac{1}{2}\sqrt{3},-\frac{1}{2},-\frac{1}{2}\sqrt{3},-\frac{1}{2}]}{\sqrt{3}}. \tag{113}$$

An orthonormal base for the phason modes, which corresponds to a relative translation of the two hexagonal lattices, is given by

$$u_{\varphi_1}^{\mathrm{T}} = \frac{[1, 0, -\frac{1}{2}, \frac{1}{2}\sqrt{3}, -\frac{1}{2}, -\frac{1}{2}\sqrt{3}]}{\sqrt{3}}, \tag{114}$$

$$u_{\varphi_2}^{\mathrm{T}} = \frac{[0, 1, -\frac{1}{2}\sqrt{3}, -\frac{1}{2}, \frac{1}{2}\sqrt{3}, -\frac{1}{2}]}{\sqrt{3}}. \tag{115}$$

As in the case of the octagonal quasipattern, under rotations the phason field $\tilde{\varphi} = (\varphi_1, \varphi_2)$ changes with five times the rotation angle.

An expansion very similar to that in the decagonal case leads to the long-wave equations

$$\partial_t \vec{\phi} = D_1 \nabla^2 \vec{\phi} + (D_2 - D_1)\nabla(\nabla \cdot \vec{\phi}), \tag{116}$$

$$\partial_t \varphi_1 = D_3 \nabla^2 \varphi_1 + (D_4 - D_3)\partial_y(\partial_y \varphi_1 + \partial_x \varphi_2), \tag{117}$$

$$\partial_t \varphi_2 = D_3 \nabla^2 \varphi_2 + (D_4 - D_3)\partial_x(\partial_x \varphi_1 + \partial_y \varphi_2) \tag{118}$$

with $\vec{\phi} = (\phi_x, \phi_y)$. Note that to this order the equation for the phase modes of the dodecagonal pattern is the same as that for an isotropic medium. The values of the coefficients are

$$D_1 = \frac{1}{4} - \frac{q^2}{u_1}, \tag{119}$$

$$D_2 = \frac{3}{4} - \frac{2q^2}{v_1} - \frac{q^2}{u_1}, \tag{120}$$

$$D_3 = \frac{1}{4} - \frac{q^2}{u_2}, \tag{121}$$

$$D_4 = \frac{3}{4} - \frac{2q^2}{v_2} - \frac{q^2}{u_2} \tag{122}$$

with $v_1 = -R[\alpha - 2R(2\beta + 2\nu + 2\gamma + 1)]$, $v_2 = -R[\alpha + 2R(2\beta + 2\gamma - 2\nu - 1)]$, $u_1 = 2R[\alpha + R(1 + \gamma - 2\beta - \nu)]$, $u_2 = 2R[\alpha + R(1 + 2\beta - \gamma - \nu)]$ and R given by Eq. (95).

In complex form the long-wave equations become

$$\partial_t \phi = D_1 |\nabla|^2 \phi + \tfrac{1}{2}(D_2 - D_1)\nabla(\bar{\nabla}\phi + \nabla\bar{\phi}), \tag{123}$$

$$\partial_t \varphi = \tfrac{1}{2}(D_3 + D_4)|\nabla|^2 \varphi + \tfrac{1}{2}(D_3 - D_4)\bar{\nabla}^2 \bar{\varphi}. \tag{124}$$

One feature that distinguishes the dodecagonal quasipattern from the octagonal and the decagonal quasipattern is the fact that its long-wave dynamics decouple into pure phase and pure phason modes. This is due to the symmetry of the dodecagonal quasipattern as has been pointed out earlier for the case of quasicrystals [28]. Thus, the eigenvalues are simply given by

$$\sigma_1 = -D_1 Q^2, \qquad \sigma_2 = -D_2 Q^2, \qquad \sigma_3 = -D_3 Q^2, \qquad \sigma_4 = -D_4 Q^2, \tag{125}$$

and one obtains separate phase and phason instabilities when $D_{1,2}$ or $D_{3,4}$ change sign, respectively. Typical stability diagrams are shown in Fig. 9. The stability limits due to phase and phason modes are indicated by dashed

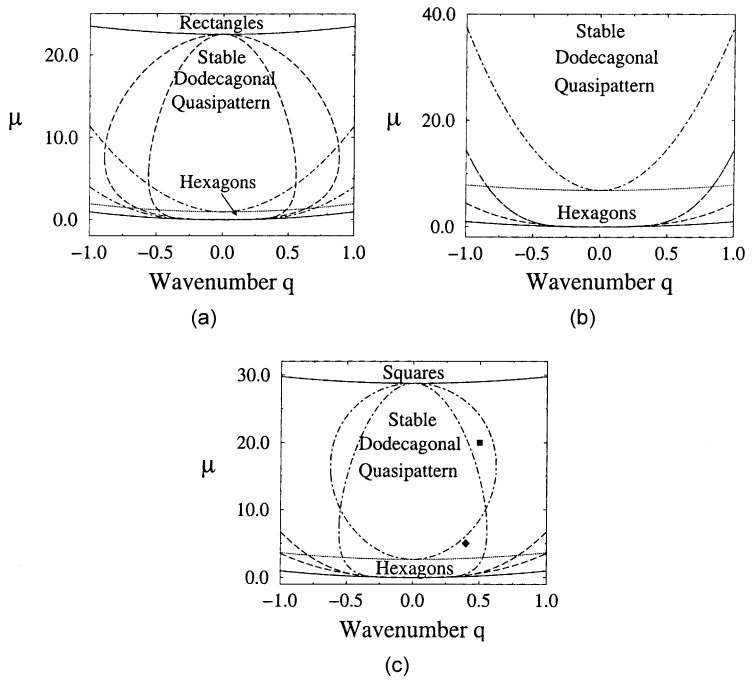

Fig. 9. Stability diagrams for $\alpha = 1$ and (a) $\nu = 0.7$, $\gamma = 0.3$ and $\beta = 0.5$, (b) $\nu = 0.9$, $\gamma = 0.8$ and $\beta = 0.4$, and (c) $\nu = 0.9$, $\gamma = 0.9$ and $\beta = 0.2$. The lower solid line corresponds to the saddle-node bifurcation of the quasipattern. In all the figures, the quasipattern is unstable at onset and becomes stable above the dotted line (cf. Eq. (104)). In (a) and (c) there is a further transition to rectangles and squares, respectively, above the upper solid line. The stable region of the quasipattern is limited by long-wave instabilities corresponding to the phase (long dashed lines) and phason modes (dash-dotted lines). The diamond and square in (c) correspond to the simulations in Figs. 10 and 11, respectively.

and dash-dotted lines, respectively. Over wide ranges of parameters the stable wavenumber band is limited by phason modes.

For the phase modes, the eigenvectors correspond to the usual irrotational and divergence free modes (equivalent to transversal and longitudinal waves in an elastic medium). They satisfy

$$\nabla \cdot \vec{\phi}_\mathrm{l} = 0, \qquad \nabla \times \vec{\phi}_\mathrm{t} = 0. \tag{126}$$

For the phason modes, on the other hand, the eigenvectors are

$$\tilde{\varphi}^{\sigma_3} = \begin{bmatrix} -Q_x \\ Q_y \end{bmatrix} \mathrm{e}^{\mathrm{i}\mathbf{Q}\cdot\mathbf{x}}, \qquad \tilde{\varphi}^{\sigma_4} = \begin{bmatrix} Q_y \\ Q_x \end{bmatrix} \mathrm{e}^{\mathrm{i}\mathbf{Q}\cdot\mathbf{x}}. \tag{127}$$

These modes satisfy the equations:

$$\partial_y \varphi_1^{\sigma_3} + \partial_x \varphi_2^{\sigma_3} = 0, \qquad \partial_x \varphi_1^{\sigma_4} - \partial_y \varphi_2^{\sigma_4} = 0. \tag{128}$$

In order to study the behavior arising from these instabilities, we have simulated numerically Eqs. (87) and (88). We start with a perfect dodecagonal quasipattern and add a perturbation in the form of $\tilde{\varphi}^{\sigma_3}$ (Fig. 10a) or $\tilde{\varphi}^{\sigma_4}$ (Fig. 11a), with $\mathbf{Q} = (4\pi/L, 4\pi/L)$. Since the perturbation is along the diagonal, the evolution of the system will be quasi-one-dimensional. This will allow us to study the sub- or supercritical nature of the bifurcation. In Fig. 10, we show the evolution of the instability corresponding to $\sigma_3 > 0$. The perturbation grows until it creates phase slips at time $t = 380$ (Fig. 10b) on a line perpendicular to the direction of the perturbation. Along that line four of the

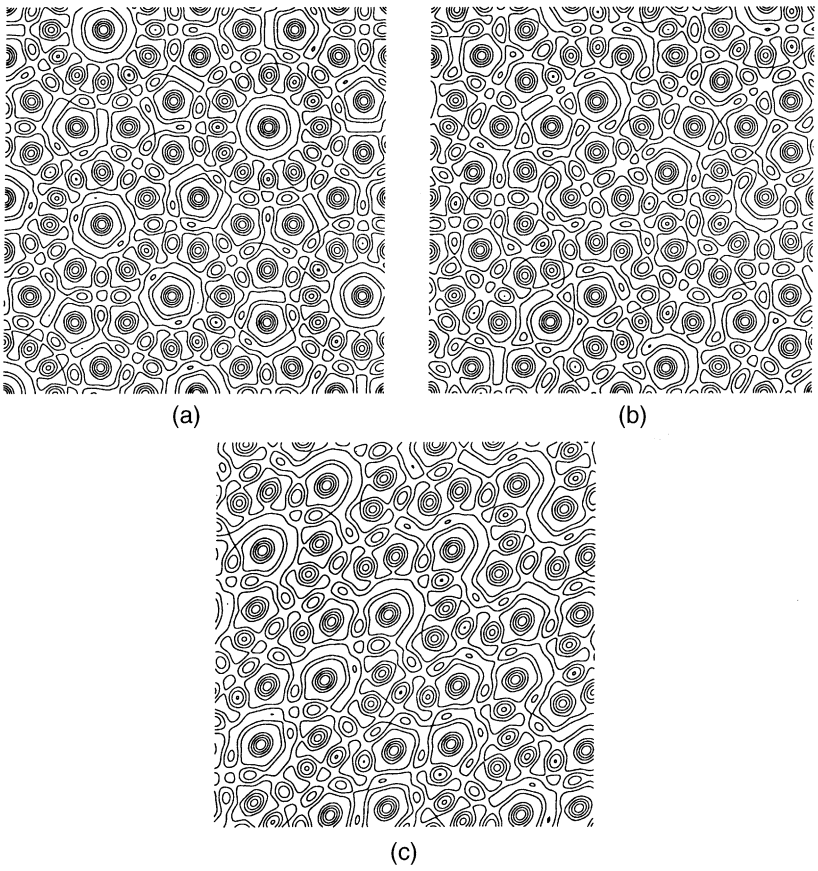

Fig. 10. Instability corresponding to $\sigma_3 > 0$ (diamond in Fig. 9c) for: (a) $t = 0$, (b) $t = 380$, and (c) $t = 450$ ($\mu = 5, \nu = 0.9$, $\gamma = 0.9, \beta = 0.2, q = 0.4, L = 50, k_c = 16k_{\min}$).

amplitudes vanish and change their wavenumber. Thus, the phase perturbation does not saturate and the instability is sub-critical. In Fig. 10c, the final state is shown, after the defects have annihilated each other in pairs. It corresponds to a slightly distorted quasipattern, with different wavenumbers in the various modes.

The instability corresponding to $\sigma_4 > 0$ is also sub-critical, generating phase slips (Fig. 11b). But for the values of the parameters in the simulation the square pattern minimizes the Lyapunov functional and it nucleates around the defects. The patches of squares grow (Fig. 11c) until they occupy the whole cell, resulting in a slightly distorted square pattern (Fig. 11d).

5. Defects

The properties of defects in the quasipatterns differ noticeably in the three cases investigated in this paper. Due to the absence of resonance terms in (1) (also to higher orders), the octagonal quasipattern can be considered as made up of four sub-lattices corresponding to the four basic wavevectors. Each of the sub-lattices has its own defects. Thus, taking into account the two possible 'charges' of the defects there are $2 \times 4 = 8$ different defects. They interact strongly with defects of the same sub-lattice via the phase. The interaction with the defects in the other sub-lattices

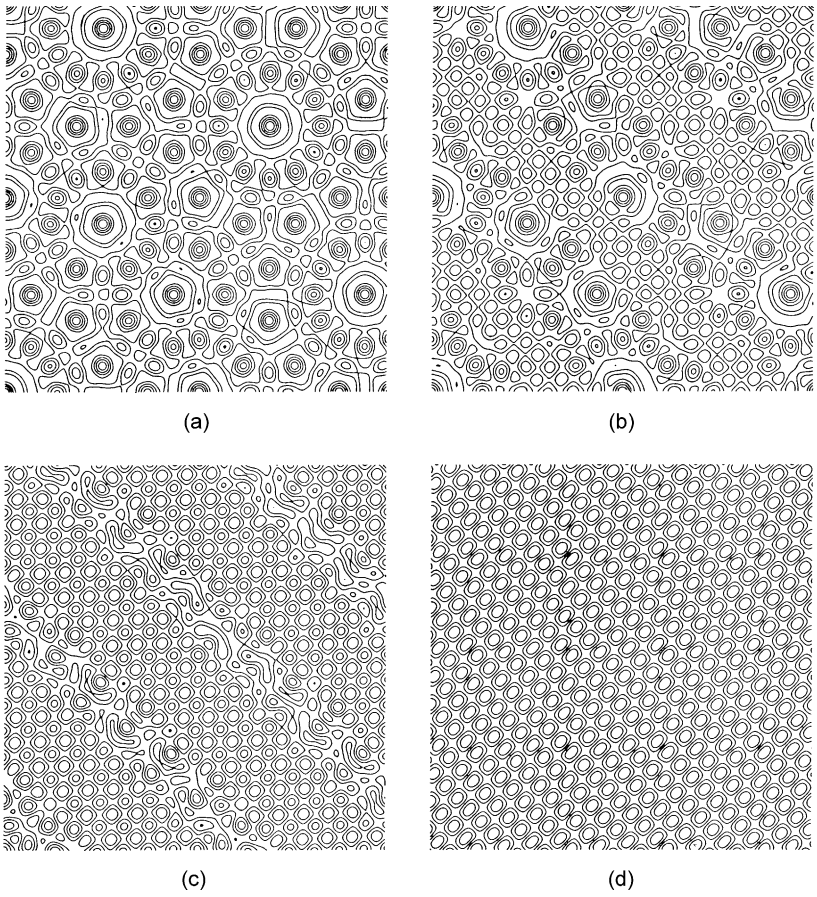

Fig. 11. Instability corresponding to $\sigma_4 > 0$ (square in Fig. 9c) for: (a) $t = 0$, (b) $t = 440$, (c) $t = 445$, and (d) $t = 600$ ($\mu = 20$, $\nu = 0.9$, $\gamma = 0.9$, $\beta = 0.2$, $q = 0.5$, $L = 25$, $k_c = 16k_{\min}$).

is only through the variations in the magnitude and is much weaker. Overall, we expect the dynamics to be quite similar to that of defects in square patterns, which are made of two rather than four sub-lattices. Topologically, two defects of different sub-lattices could bind to form a vectorial defect (cf. [29]). However, in our simulations we have not observed such kind of defects in the octagonal quasipattern. This seems to be consistent with simulations of the vector complex Ginzburg–Landau equation, where vectorial defects were never observed in the potential limit [30].

For the dodecagonal quasipatterns, the Ginzburg–Landau equations (87) and (88) have (quadratic) resonance terms coupling the three modes in each of the two hexagonal sub-lattices. At the defects, therefore, two amplitudes in the same sub-lattice must vanish leading to penta–hepta defects very similar to those in the usual hexagonal patterns. However, while in the core of penta–hepta defects of hexagons the pattern corresponds to the roll pattern, it corresponds in the dodecagonal case to the one-dimensional quasipattern. As in the hexagonal case, each penta–hepta defect carries two opposite charges corresponding to the two vanishing amplitudes. This leads to a total of $2 \times (3 \times 2) = 12$ different defects. While in the octagonal case collisions between defects can only annihilate them or leave them unchanged, collisions between penta–hepta defects can change their type. An example of such a collision is

given by the process

$$(+,-,0;0,0,0)+(-,0,+;0,0,0)\rightarrow(0,-,+;0,0,0). \tag{129}$$

Here $+/-$ in the ith entry stands for a defect with positive/negative charge in the mode A_i, while 0 indicates that the corresponding amplitude has no defect. The semicolon separates the two hexagonal sub-lattices. While there are a number of different such type-changing collisions, a penta–hepta defect in one sub-lattice can never change into one in the other sub-lattice, since there is no resonance term in (87) and (88) involving modes of both hexagonal sub-lattices. In other words, there is no penta–hepta defect that has one vanishing amplitude in one sub-lattice and one vanishing amplitude in the other sub-lattice.

Penta–hepta defects within the same sub-lattice interact with each other strongly through the phase. The strength of the interaction (attraction vs. repulsion) is expected to be related to the sum N of the products of the charges of the individual defects [31]

$$N=\sum_{j=1}^{n}\delta_j^1\delta_j^2. \tag{130}$$

Here $\delta_j^{1,2}$ is the topological charge of the first and second defect, respectively, in the mode A_j. For hexagons ($n=3$), N can only take on the values -2, -1, 1, and 2, since for any defect pair there is always a mode that vanishes in both of them. Thus, within each sub-lattice all penta–hepta defects interact strongly. Penta–hepta defects of different sub-lattice will interact only weakly (through the magnitude). Considering that collisions do not change defect type across the sub-lattices, one may expect the ordering dynamics that leads from disordered patterns to ordered quasipatterns to occur in the two sub-lattices essentially independently.

The decagonal case appears to be the most interesting one in terms of the defect dynamics. As in the case of defects in hexagon patterns, the (quartic) resonance term requires that in a defect two amplitudes vanish. In contrast to the hexagonal or dodecagonal case there are, however, two qualitatively different defect types. In one of them, the vanishing Fourier modes are rotated by $2\pi/5$ with respect to each other, while in the other they are rotated by $2\times 2\pi/5$. While in the former case the core exhibits the quasipattern H_2, it is the quasipattern H_1 that appears in the latter case (cf. Fig. 5d and e). Examples of the two cases are shown in Fig. 12a and b. Overall, there are $5\times 4=20$ different defects.

The same arguments employed in the hexagonal case [31] suggest that the interaction between defects is richer in the decagonal quasipattern than in hexagons or in the other quasipatterns investigated in the present paper. In hexagonal or dodecagonal patterns two penta–hepta defect pairs always share a mode that vanishes in both pairs and the charge product N given by (130) never vanishes, implying that the defects always interact strongly through the phase. In the decagonal quasipattern, however, the analogously defined N (with $n=5$) can also take the value 0, since two pairs of defects need not share a mode with vanishing amplitude. The above argument therefore suggests that in this case the interaction is very weak. We have confirmed this expectation by numerical simulations of the Ginzburg–Landau equations (41). While defect pairs that share a vanishing amplitude ($N\neq 0$) attract or repel each other quite strongly, those with $N=0$ move so slowly that our preliminary simulations were not able to identify even whether their interaction is attractive or repulsive.

A separation into weak and strong interaction also arises in the dodecagonal quasipattern. There, however, the division between strong and weak is parallel to the division into the two sub-lattices. In the decagonal case, however, the resonance term involves all modes and the quasipattern cannot be viewed as the combination of two separate sub-lattices. Correspondingly, a defect of one type can change into a defect of any other type through collisions with suitable other defects. We expect that the exceedingly weak interaction of defect pairs with $N=0$ may slow down the evolution from disordered or random initial conditions towards an ordered quasipattern.

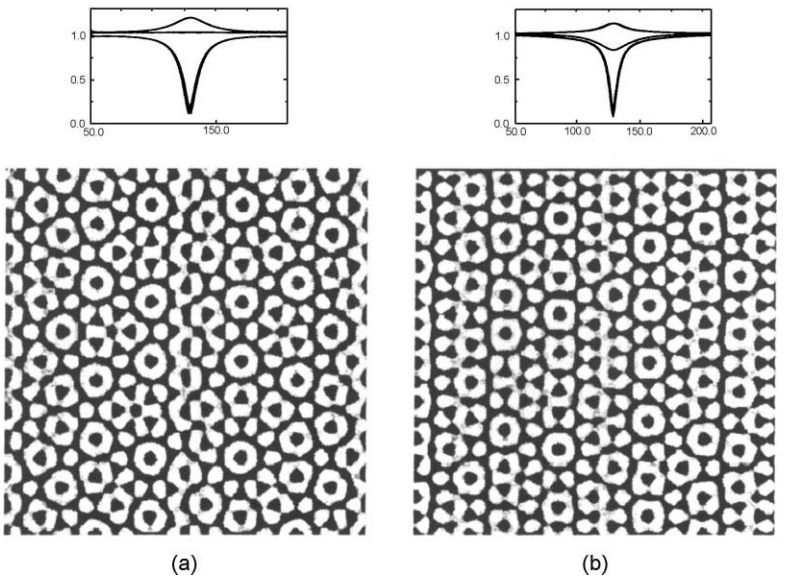

Fig. 12. Decagonal quasipattern with a defect of type (a) H_1, and (b) H_2 in the center. The top panels show a cross-section of the five amplitudes in the x-direction. Two of them vanish at the core of the defect. Of the remaining three, two are equal, as expected from Eqs. (46) and (48). In the bottom panels, a reconstruction of the physical field ψ is shown. At the core of the defects, the one-dimensional quasipatterns H_1 and H_2 can be observed (compare with Fig. 5d and e).

6. Conclusions

In this paper, we have addressed the stability of various types of quasipatterns with respect to long-wave sideband instabilities. For quasipatterns with octagonal, decagonal, and dodecagonal rotational symmetry, we have derived from the corresponding Ginzburg–Landau equations long-wave equations for the two phase and the two phason modes. Their stability analysis yields the long-wave stability properties of these patterns.

For the octagonal and the decagonal quasipatterns the phase and the phason modes are coupled and one cannot clearly separate the instabilities in those of the phases and those of the phasons. In these cases our numerical simulations suggest that the nonlinear behavior arising from the instabilities is the same as that observed in the usual Eckhaus instability. Thus, the instabilities do not saturate within the long-wave equations and lead to the creation of defect pairs which subsequently annihilate each other yielding a stable quasipattern with slightly modified wavevectors. Interestingly, however, in the dodecagonal quasipatterns the phase and phason equations decouple and there are parameter regimes in which the quasipatterns first becomes unstable with respect to phason modes rather than phase modes. The ensuing dynamics appear to be somewhat different than for the usual phase modes. This question has, however, not been pursued in detail in this paper.

The interaction between defects of the decagonal quasipattern can be extremely weak for certain combinations of defects. We expect that this will have a strong influence on the evolution from disordered initial conditions to the regular quasipattern. The investigation of the evolution can most likely not be addressed within the Ginzburg–Landau equations (41) since the ordering dynamics will also entail a spreading of the modes in Fourier space along the critical circle (cf. the dynamics found in hexagon patterns with rotation [32]). This will necessitate the use of suitable equations of the Swift–Hohenberg type.

There are other questions, such as the far-field phase configuration associated with the defects, as well as analytical expressions for their mobility and interactions, that have not been addressed in the current paper. It should be noted that the deformations associated with dislocations and disclinations, as well as their interaction energy, have already been calculated in the case of quasicrystals [33,34]. How these results apply to the current case of quasipatterns is beyond the scope of the present work.

Acknowledgements

We gratefully acknowledge discussions with J. Viñals, L. Kramer, M. Silber, and M.R.E. Proctor, who pointed out an omission in our earlier results for the zig-zag instability of octagonal quasipatterns. This research was supported by NASA (NAG3-2113), the Engineering Research Program of the Office of Basic Energy Sciences at the Department of Energy (DE-FG02-92ER14303) and a grant from NSF (DMS 9804673).

References

[1] D. Shechtman, I. Blech, D. Gratias, J. Cahn, Phys. Rev. Lett. 53 (1984) 1951.
[2] B. Malomed, A. Nepomnyashchy, M. Tribelsky, Sov. Phys. JETP 69 (1989) 388.
[3] B. Christiansen, P. Alstrom, M. Levinsen, Phys. Rev. Lett. 68 (1992) 2157.
[4] W. Edwards, S. Fauve, Phys. Rev. E 47 (1993) 788.
[5] E. Pampaloni, P.L. Ramazza, S. Residori, F.T. Arecchi, Phys. Rev. Lett. 74 (1995) 258.
[6] A. Golovin, A. Nepomnyashchy, L. Pismen, Physica D 81 (1995) 117.
[7] D. Walgraef, N.M. Ghoniem, J. Lauzeral, Phys. Rev. B 56 (1997) 15361.
[8] A. Kudrolli, B. Pier, J. Gollub, Physica D 123 (1998) 99.
[9] H. Arbell, J. Fineberg, Phys. Rev. Lett. 81 (1998) 4384.
[10] H. Arbell, J. Fineberg, Phys. Rev. Lett. 84 (2000) 654.
[11] N.D. Mermin, S.M. Troian, Phys. Rev. Lett. 54 (1985) 1524.
[12] R. Lifshitz, D. Petrich, Phys. Rev. Lett. 79 (1997) 1261.
[13] M. Silber, C. Topaz, A. Skeldon, Physica D 143 (2000) 205.
[14] H. Müller, Phys. Rev. E 49 (1994) 1273.
[15] W. Zhang, J. Viñals, Phys. Rev. E 54 (1996) 4283.
[16] W. Zhang, J. Viñals, J. Fluid Mech. 336 (1997) 301.
[17] P. Chen, J. Viñals, Phys. Rev. E 60 (1999) 559.
[18] S. Residori, et al., Phys. Rev. Lett. 76 (1996) 1063.
[19] E. Pampaloni, S. Residori, S. Soria, F. Arecchi, Phys. Rev. Lett. 78 (1997) 1042.
[20] L. Pismen, B. Rubinstein, Chaos, Solitons and Fractals 10 (1999) 761.
[21] R. Herrero, E. Grobe Westhoff, A. Aumann, T. Ackemann, Yu.A. Logvin, W. Lange, Phys. Rev. Lett. 82 (1999) 4627.
[22] B. Dionne, M. Silber, A. Skeldon, Nonlinearity 10 (1997) 321.
[23] M. Silber, M.R. Proctor, Phys. Rev. Lett. 81 (1998) 2450.
[24] C. Hu, R. Wang, D. Ding, Rep. Prog. Phys. 63 (2000) 1.
[25] A. Newell, J. Whitehead, J. Fluid Mech. 38 (1969) 279.
[26] R. Hoyle, Physica D 67 (1993) 198.
[27] M. Golubitsky, J. Swift, E. Knobloch, Physica D 10 (1984) 249.
[28] J. Socolar, Phys. Rev. B 39 (1989) 10519.
[29] L. Pismen, Physica D 73 (1994) 244.
[30] E. Hernández-García, M. Hoyuelos, P. Colet, M.S. Miguel, Phys. Rev. Lett. 85 (2000) 744.
[31] L. Tsimring, Physica D 89 (1996) 368.
[32] B. Echebarria, H. Riecke, Physica D 139 (2000) 97.
[33] P. De, R.A. Pelcovits, Phys. Rev. B 35 (1987) 8609.
[34] P. De, R.A. Pelcovits, Phys. Rev. B 38 (1988) 5042.